Theor Chem Acc (2012) 131:1268
DOI 10.1007/s00214-012-1268-x

REGULAR ARTICLE

Theoretical analysis of charge-transfer electronic spectra of methylated benzenes—TCNE complexes including solvent effects: approaching experiment

Pavel Mach · Šimon Budzák · Miroslav Medveď · Ondrej Kyseľ

Received: 24 May 2012 / Accepted: 18 August 2012 / Published online: 11 September 2012

Abstract The paper brings new accurate theoretical description of charge-transfer (CT) electronic spectra of a complete series of methylated benzenes–tetracyanoethylene (*N*MB-TCNE) complexes and detail comparison with complete experimental data both in the gas phase and in polar media. It is shown that the energies of the first two (CT) absorption transition in these intermolecular EDA (electron donor–acceptor) complexes are described well by the CC2/aug-cc-pVTZ method. In agreement with experimental data, it reproduces well both the bathochromic shift of the two π(NMB) $\rightarrow$ π^*(TCNE) transitions (ranging from 3.41 to 2.23 eV) with the increasing number of methyl groups *N* as well as the value of splitting between them. Nevertheless, the CC2 transitions are systematically smaller, that is, red-shifted, with respect to experimental quantities in the gas phase by ca. 0.15–0.2 eV, which is an inaccuracy of the CC2 approach. The TD-LC-BLYP method better describes studied CT transitions than PBE0 or B3LYP functionals; however, the transition energies are too sensitive to the fitting range separation factor μ. The PCM solvation model combined with the CIS or LC-BLYP methods predicts red solvent shifts for all the studied CT transitions in *N*MB-TCNE complexes due to a larger stabilization of the excited states compared to their ground states in the solvent. The stabilization increases with solvent polarity and decreases with increasing *N*. The CIS/PCM solvent shifts are smaller than experimental values (taken as the difference for the gas phase and the polar CH_2Cl_2 solvent) by 0.1–0.15 eV, that is, by 30–40 %, however, being more consistent than those obtained by TD-DFT functionals used. Experimentally interesting (hexamethylbenzene)$_2$-TCNE complex (2:1) was also studied by the LC-BLYP approach. The exciton splitting together with the bathochromic effect on absorption in comparison with 1:1 complex was found.

Keywords Charge-transfer complex · Excitation energy · CC2 · Solvent effect

1 Introduction

Photophysical and photochemical properties of charge-transfer (CT), or electron donor–acceptor (EDA), complexes have been of interest for a long time mainly due to their wide spectrum of applications ranging from chemistry, material science, and medicine to biology [1–3]. The CT interactions, particularly those between aromatic electron acceptors and various electron donors containing nitrogen, oxygen, or sulphur atoms, play a leading role in many organic and inorganic reaction mechanisms as well as biological processes. While in organic chemistry, the CT complexes act as intermediates in a wide variety of reactions involving nucleophiles and electron acceptor molecules [4], they are also operative in various biologically important macromolecular assembly processes such as, for

Electronic supplementary material The online version of this article (doi:10.1007/s00214-012-1268-x) contains supplementary material, which is available to authorized users.

P. Mach (✉)
Department of Nuclear Physics and Biophysics,
Faculty of Mathematics, Physics and Informatics,
Comenius University, Mlynská dolina F1,
84248 Bratislava, Slovak Republic
e-mail: mach@fmph.uniba.sk

Š. Budzák · M. Medveď · O. Kyseľ
Department of Chemistry, Faculty of Natural Sciences,
Matej Bel University, Tajovského 40,
97400 Banska Bystrica, Slovak Republic

example, protein folding [4–10]. From a technological point of view, they need to be considered in many practical aspects of designing opto-electronic materials and devices [11]. Rapid chemical analyses via formation of CT complexes (e.g., between TCNE as an acceptor and different drugs) [12, 13] are also a good reason for a deeper study of their properties by adequate theoretical approaches.

Over the years, a very large number of CT complexes have been prepared and experimentally studied. Research interest in complexes between methyl-substituted benzene and TCNE has recently been revived mainly due to a possibility to systematically study a set of EDA complexes with the increasing charge transfer (with increasing *N*) by accurate theoretical methods and modern experimental techniques [14–17].

A particular problem of importance is the complex conformation in the ground state. Many molecular complexes cannot be fully isolated and so must be studied in solution or crystals. There has been considerable discussion about the relative orientation of the donor and acceptor components in certain D-A complexes in solution, with conflicting data reported, and the question about the exact geometry of the complexes still remains open [1]. Moreover, electronic spectra of some CT complexes contain two or more bands close to each other what can be associated with transitions from degenerated or near degenerated highest occupied orbitals of D to the lowest unoccupied orbitals of A, but also with the existence of two (or more) distinct complex geometries.

The simplest way to treat excited states at the correlated level is CIS(D) [18], which can be viewed as the most straightforward and computationally efficient generalization of the CIS method introducing approximately (up to the second order) the effect of double excitations (with accuracy and computational demands comparable to the MP2 ground-state energy calculation). There are also another methods having this property, among them probably the most popular being CC2 [19]. Owing to an efficient implementation in the resolution of identity (RI) approximation of Hättig and Weigend [20], the CC2 method can be used as a reference method to calculate electronic spectra even of relatively large systems. An efficient way to move closer to experimental absorption spectra is to use spin scaled (SCS) versions of these methods—SCS-CC2 [21] and SCS-CIS(D) [22, 23] or multireference methods such as, for example, CASPT2.

A comparable accuracy can also be reached by the second-order algebraic-diagrammatic construction (ADC(2)) approximation within the polarization propagator formalism [24]. A more demanding CASPT2 approach correcting the complete active space SCF (CASSCF) method for dynamic correlation to the second order is usually used for smaller systems to approach experimental CT spectra in the gas phase.

During the last years, a significant amount of works using time-dependent density functional theory (TD-DFT) approaches to calculate transition energies of large molecular complexes frequently used in material sciences or molecular biology were published. Although the TD-DFT methods based on local density approximation (LDA), generalized gradient approximation (GGA), or hybrid functionals are usually not able to properly describe CT excited states, several attempts have recently been made to overcome this problem. While one group relies on the correction of the long-range (LR) part of the exchange potential such as, for example, in the long-range corrected BLYP (LC-BLYP) method (see Computational details), the second successful approach is based on the double-hybrid DFT functionals as proposed and applied to electronic transitions of both smaller and larger molecular systems by Grimme et al. [25]. Due to semiempirical nature of DFT functionals, their applications should be verified by reliable non-empirical methods, or experimental data, especially for compounds or intermolecular complexes like ours which are characterized by almost complete electron transfer in their excited states. In this context, let us mention that, the ADC(2) approach was used to calculate electron transitions in stacked nucleobase dimer complexes by Hobza et al. [26].

The reliability of less demanding methods opens the door to the investigation of larger systems in the gas phase, but also molecules and their complexes in the condense media, where too sophisticated approaches cannot yet be straightforwardly applied. The demand to study CT complexes in either nonpolar or, more frequently, in polar solvents arising mainly (but not only) from a prevailing body of experimental electronic and vibrational spectra is undisputable. In this context, the computationally very versatile PCM (polarizable continuum model) method is being intensively developed refined and significantly improved [27–29]. Its extension to electronic excited states [30–34] is important not only because of their study in steady-state conditions, but perhaps predominantly due to a possibility to study solvation dynamics (e.g., inertial and diffuse responses of the solvent) of these states [35]. The PCM/CIS and PCM/TD-DFT approaches are being at present widely applied to electronic absorption and emission processes in various complex systems in solvents. In our present study, we contribute to further testing of their accuracy and reliability as well as to deeper understanding of electronic transitions in CT complexes, namely in a series of methyl-substituted benzenes with TCNE, for which complete experimental data both in the gas phase and in the polar solvents are available.

2 Computational details

According to our previous experience with *N*MB-TCNE complexes, all systems have been optimized at the B97-D

[36] level of theory using the 6-311+G(2d,p) basis set. In order to test the local minima character of the obtained stationary points, we carried out frequency calculations. Using the optimized structures, excitation energies of the first two excited states were computed by means of the CIS, CIS(D), CC2, CASSCF, and CASPT2, as well as TD-DFT methods. Based on the work by Jacquemin [37], the 6-311+G(2d,p) basis set was also used for the TD-DFT excited state calculations as a reasonable compromise between the quality and computational demands. In the case of the CC2 method, a set of standard non-augmented as well as augmented Dunning's correlation consistent basis sets (cc-pV*X*Z, respectively, aug-cc-pV*X*Z with $X = D$, T, and Q) was utilized with appropriate auxiliary basis set [38]. Extrapolation to the complete basis set (CBS) limit was done using a well-known $1/X^3$ dependence on the basis set cardinal number [39].

A particular attention in our analysis is given to the assessment of the accuracy of selected hybrid and LR-corrected DFT methods. It is well known that standard (LDA and GGA) DFT methods tend to perform poorly in a number of important applications. In the context of our study, let us mention a poor prediction of chemical properties of molecules that contain high-electronegativity atoms [40], a poor description of charge-transfer excitations [41, 42], and also the poor polarizabilities of π-conjugated molecules [43]. These failures have been thoroughly analysed, and they were attributed to an incorrect asymptotic behaviour of the exchange–correlation part of the DFT functionals [44]. A promising way to improve DFT description has been keeping DFT-like short-range (SR) exchange while switching to the HF exchange smoothly at longer distances. There are several implementations of this basic idea. In our study, we employ the LR-corrected functional LC-BLYP proposed by Iikura et al. [45] which was shown [46, 47] to provide reasonably accurate CT excitation energies of conjugated molecules.

For the interpretation of ionization potentials (IPs), Koopmans' theorem [48], equating the IP with the negative value of the energy of the molecular orbital from which the electron is removed, is usually used. However, in many cases, this method fails to provide the quantitative IPs correctly, or even to reproduce the correct orbital ordering. Cederbaum and co-workers [49, 50] devised so-called OVGF technique, in which many-body perturbation theory is used to derive the equations that enable us to calculate IPs including corrections for electron correlation and for orbital relaxation effects. This method was used also in this study for calculation of valence ionization potentials of respective donors.

The PCM [29, 51] calculations have been done according to [52], that is, the IEF version of PCM approach. For all PCM calculations, default settings as defined in Gaussian09 implementation [53] were used: the cavity is constructed from interlocking spheres, centred on atoms and having UFF atomic radii [54] scaled by a factor 1.1. Hydrogen atoms have individual spheres. Sphere tessellation uses the Lebedev-Laikov grid with average density of five points per $Å^2$. The continuous surface charge formalism is used as described in [52]. Nonequlibrium polarizable continuum model in combination with the CIS and LC-BLYP methods enabled us to treat solvent effects on vertical excitation energies [55]. Geometry optimizations, vibrational frequency calculations, and OVGF ionization energy calculations were performed using Gaussian09 [53], TD-DFT calculations by Gamess [56] quantum chemistry software. CC2 calculations were done in Turbomole version 5.10 [57], and CASSCF and CASPT2 were done in Molcas version 7.1 [58].

3 Results and discussion

3.1 Geometry optimization and interaction energies of NMB-TCNE complexes

The optimization of geometry of all seven studied *N*MB-TCNE complexes has shown that each of them has two local energy minima (corresponding to structures referred to as I and II in Scheme 1, with I being always global minima—see also Electronic supplementary material for structures of all studied complexes) which are very close in energy (differing from each other at the most 0.7 kcal/mol for the Mesitylene-TCNE complex) and qualitatively correspond to maximum overlap between each of two perpendicular π-HOMOs of *N*MB and LUMO orbital of TCNE. We also performed calculations (geometry optimization and/or single-point calculation) in polar solvent (e.g., CH_2Cl_2), and we did not find any substantial change from gas phase results in structure of ground state, for the mentioned minima I and II. The structure **I** remain also in a solvent to be the global minimum (e.g., the difference in energy between I and II structures is 0.6 kcal/mol in CH_2Cl_2 for the Mesitylene-TCNE complex). The respective distances between the planes of particular *N*MB and that of TCNE are denoted as *R*(I) and *R*(II) (see Fig. 1). As expected, both values decrease with the increasing number of methyl groups *N*; though with larger *N* values, the decrease is less pronounced, which is caused by increased nonbonding repulsion between the methyl groups and TCNE molecule. Due to this repulsion, the TCNE molecule does not remain planar, but with increasing *N*, the CN groups become increasingly distorted in direction of the out-of-plane vibrational mode (see paper [16]).

The B97-D and CC2 (identical to MP2 and BSSE corrected) interaction energies of *N*MB-TCNE complexes are

both strictly linearly dependent on number N with very similar slopes (see Fig. 2). However, the CC2 values are ca. 20 % larger (in absolute value) than the B97-D energies. Benchmark calculations of the intermolecular interaction energies of aromatic molecules show that the MP2 method at the basis set limit (reached by extrapolation or using R12 approach [59]) overestimates the attraction compared with the more reliable CCSD(T) method [60–62]. As a practically useful though empirical fact, Antony and Grimme [63] found that a one-electron basis set of triple-zeta quality lacking diffuse functions performs well for non-covalent binding energies at MP2 level, with the remaining basis set superposition error (BSSE) and incompleteness error largely cancelling. From the latest research by Hobza et al. [64], it follows that this overestimation of dispersion at the MP2 level is not general, but it is characteristic for pi–pi interacting systems, contrary to interactions of saturated chains. Our CCSD(T) (BSSE corrected) study using the 6-311+G(2d,p) basis set shows, indeed, that the interaction energy for Benzene-TCNE (B-TCNE) complex lies somewhat above CC2 and B97-D values but closer to the latter (see Fig. 2). This fact indicates that the B97-D interaction energies of CT complexes can be taken with confidence.

3.2 Methodology of testing calculations for Benzene-TCNE complex in the gas phase

Accurate description of electronic transitions with significant CT character for larger molecular systems such as EDA complexes is methodologically and computationally a challenging task. *N*MB-TCNE complexes are known to have almost complete electron transfer in the two lowest electronic excited states. For testing calculations, we used following ab initio methods CIS, CIS(D), CASSCF, CASPT2, and CC2 along with TD-DFT based on both LR-uncorrected (BLYP, B3LYP, and PBE0) as well as LR-corrected DFT functionals (LC-BLYP). The results for the first allowed electronic transition energy in the B-TCNE complex are given in Table 1. It can be seen that inclusion of double excitations in CIS(D), CASSCF, CASPT2, and CC2 is crucial, and all these approaches give consistent

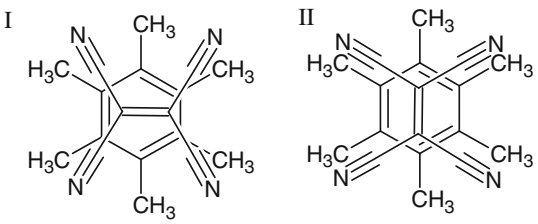

Scheme 1 Two local minima of *N*MB-TCNE complexes presented on the example of hexamethylbenzene

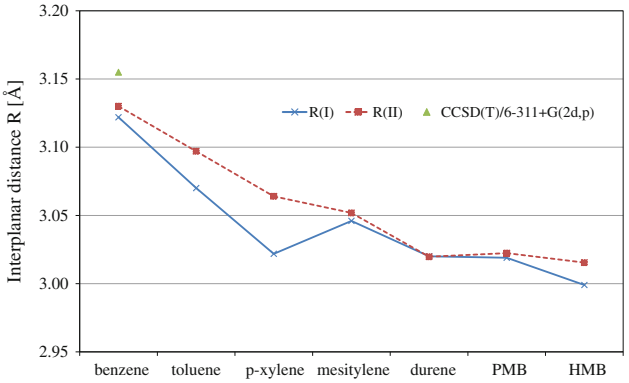

Fig. 1 Interplanar distance R for *N*MB-TCNE complexes obtained at the B97-D/6-311+G(2d,p) level. R(I) and R(II) values correspond to respective minima—see Scheme 1. All values are in 10^{-10} m. For B-TCNE, the CCSD(T)/6-311+G(2d,p) result is also shown

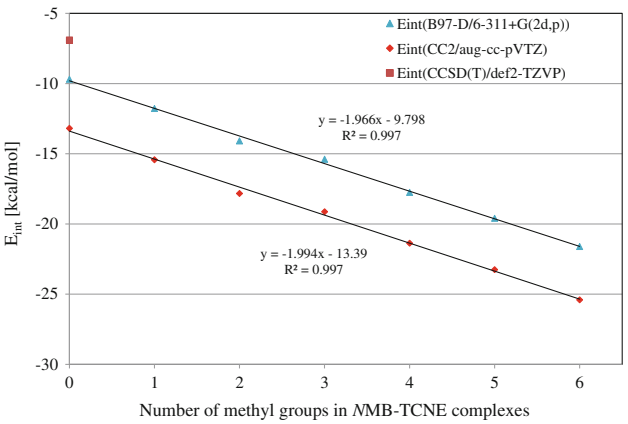

Fig. 2 Dependence of CC2 (MP2)/aug-cc-pVTZ and B97D/6-311+G(2d,p) interaction energies on number of methyl groups in *N*MB-TCNE complexes. For B-TCNE, the CCSD(T)/def2-TZVP result is also shown

results ranging from 340 to 390 nm (i.e., the differences are less than 0.5 eV), with the CIS(D) value (3.16 eV) being the furthest from the gas-phase experimental value (3.59 eV). Almost perfect match with the experiment was obtained with CASPT2 (3.64 eV), though we note that the basis set used was not yet fully saturated. As mentioned before, the RI-CC2 approach is generally accepted as an appropriate method to calculate CT electronic transitions in large molecular systems. This statement is in line with our findings: the CC2 values range from 3.36 to 3.42 eV weakly depending on basis sets used. However, we are aware of the fact that since, in B-TCNE complex, the CC2 transition energy is smaller than experimental value by 0.15–0.2 eV, so it would be found with other XMB-TCNE complexes. We thus regard the CC2 approach as a good ab initio compromised method to treat all here studied complexes on equal footing.

In order to assess the basis set effects, we have tested the influence of three basis set groups (particularly defined also by cardinal number X) on the CC2 excitation energy (see Table 1; Fig. 3). Figure 3 depicts the dependences of $1/X^3$ for X approaching infinity. It can be seen that increasing the basis set size leads to a decrease of the excitation energy with the least pronounced dependence for the aug-cc-pVXZ series. The dependences have almost the same extrapolated value of the transition energy equal to 3.34 eV (371 nm). This value is relatively close to experiment which is 3.59 eV (345 nm) in the gas phase; nevertheless, for our further analysis, it is important to keep in mind that the difference is still non-negligible (0.25 eV). One can note that aug-cc-pVTZ provides satisfactorily accurate results compared to the CBS limit with the difference between them being less than 0.1 eV.

The obtained CIS excitation energies are of course too large, which is a well-known fact [65].

We report these values in the context of our investigation of solvent effects (see Sect. 3.6), which can be straightforwardly obtained within the PCM model by the CIS/PCM calculations.

DFT results presented in Table 1 document a significant influence of better description of long-range (LR) exchange interactions in the LC-BLYP method on the first excitation energy in B-TCNE compared to uncorrected methods.

Table 1 Excitation energy of the first singlet allowed state $^1A_1$ for Be-TCNE complex calculated with selected methods

Method/basis set	Gas phase	
	λ (nm)	E (eV)
Experiment in gas phase [75]	345	3.59
Experiment in CH_2Cl_2 [69]	385	3.22 (0.37)[a]
CIS/6-311++G(2d,2p)	295	4.20
CIS/aug-cc-pVTZ	293	4.23 (0.20)[b]
CIS(D)/cc-pVTZ	389.7	3.18
CIS(D)/6-311++G(2d,2p)	392.8	3.16
CASSCF(6,6)/6-311+G(2d,p)	359	3.45
CASPT2(6,6)/6-311+G(2d,p)	341	3.64
CC2/6-311++G(2d,2p)	366.5	3.38
CC2/aug-cc-pVTZ	368.0	3.37
CC2/aug-cc-pVQZ	369.5	3.36
CC2/def2-QZVPP	368.6	3.36
TD RI-BLYP/6-311+G(2d,p)	583	2.13
TD B3LYP/6-311+G(2d,p)	514	2.41
TD PBE0/6-311+G(2d,p)	487	2.55
TD B2 PLYP/6-311+G(2d,2p)	454	2.73
TD-LC-BLYP/6-311+G(2d,p)[c]	357	3.47

[a] Value in parentheses is experimental red solvent shift

[b] CIS PCM/aug-cc-pVTZ value of red solvent shift

[c] Range separation factor $\mu = 0.33$

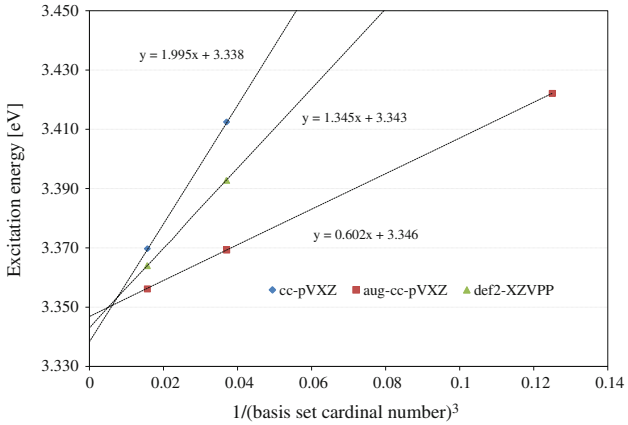

Fig. 3 Dependence of the CC2 excitation energy for the $^1A_1$ state of B-TCNE on $1/X^3$ for cc-pVXZ, aug-cc-pVXZ, and def2-XZVPP basis sets

While the GGA-BLYP as well as the hybrid B3LYP and PBE0 methods predict too low excitation energies ranging from 2.13 to 2.55 eV, LR-corrected version of BLYP gives 3.47 eV (357 nm) in a good agreement with the experiment. The failure of the LR-uncorrected approaches come from the fact that the LR exchange interactions are important when too different electron distributions in the ground and excited states occur. The PBE0 parameterization can partly solve the problem providing an acceptable agreement with experimental spectra of many aromatic compounds and their derivatives. However, in the case of strong electron transfer excitations, which occur in π-EDA complexes, this functional is not accurate. As a measure of the change of charge distribution connected with the electronic excitation, Peach et al. [66] introduced Λ parameter as the sum of the spatial overlaps between occupied and virtual orbitals involved in the excited state, weighted by the square of their transition amplitudes. Particularly, for PBE and B3LYP methods, they have concluded that significant errors can be obtained provided Λ is smaller than 0.4 and 0.3, respectively. In our case, the Λ parameter calculated for B-TCNE complex is 0.315, so the large errors of LR-uncorrected DFT excitation energies (PBE0 and B3LYP) compared to experiment are in line with these findings.

Based on the acceptable result of the LC-BLYP method (with the range separating factor μ equal to 0.33), one could conclude that this relatively inexpensive approach could be a choice for further investigation of CT excitations, particularly, in *N*MB-TCNE complexes.

Based on our assessment of methods and basis set effects, we can summarize that for accurate evaluation of transition energies for excited states with pronounced CT character (close to complete electron transfer), at least the following conditions should be fulfilled:

1. A basis set of VTZ (valence triple-zeta) quality with polarization and diffuse functions has to be used.
2. The double excitations must be included in treatments of both ground and excited states to account for the main part of electron correlation effects.
3. From a point of view of computational demands and thus applicability to larger molecular systems, the CC2 approach is recommended and was used throughout this work, though we are aware of some small systematic inaccuracy as mentioned above.

Though recently emerging TD double-hybrid (DH) DFT method [25] for treatment of excited states in isolated molecules showed quite promising performance, our results for benzene-TCNE intermolecular charge-transfer excitation (B2 PLYP/6-311+G(2d, 2p) level) give first transition energy 2.73 eV, while experimental value is 3.59 eV and our CC2 value in the same basis is 3.38 eV. Thus, inter-molecular charge-transfer excitations might be a challenge for the DH-DFT methods. As to TD-DFT methods, the LC-BLYP approach still could be a choice for the investigation of CT transitions in larger molecular complexes.

3.3 CC2 transition energies and the splitting of the first two transitions in NMB-TCNE complexes

In this paper, we treat predominantly electronic absorption spectra of *N*MB-TCNE complexes. It is well known that the first two transitions are accompanied by electron excitation from the two highest π-MO located on the benzene moiety to π*-LUMO located on TCNE. The two π-HOMOs are degenerated in benzene, mesitylene, and hexamethylbenzene (HMB) donor molecules due to their symmetry. However, in other methylated benzenes, this degeneracy is removed and the CT transitions in their complexes are significantly split. CC2/aug-cc-pVTZ results (Fig. 4) nicely confirm this fact in a good correspondence with experimental data measured in the gas phase. The CC2 results are almost strictly parallel to experimental data, being shifted to lower values by a constant average of ca. 0.2–0.15 eV (see Fig. 4) as we have anticipated just above. This is a handicap of the CC2 method. Further, one can also observe the decrease of energy of both transitions with the increase of degree of methylation *N*. This is due to a well-known electron-donating effect of methyl groups which increases the energy of both π-HOMOs in corresponding methylbenzenes, however, in different extent. The magnitude of splitting of the first two transitions is also successfully described by this theoretical method. Among some minor discrepancies belongs, a small calculated splitting for both mesitylene and HMB complexes. It is difficult to give a definite explanation of this fine effect: it

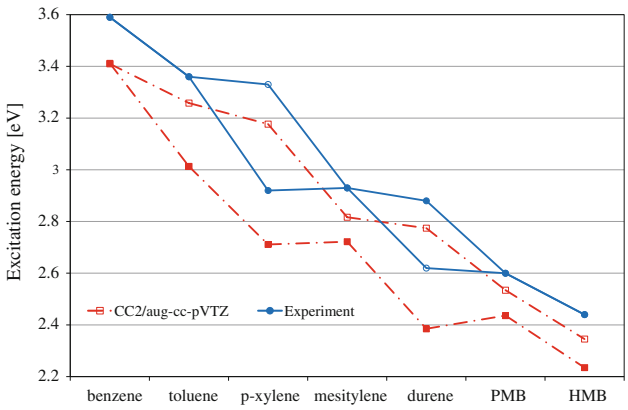

Fig. 4 CC2/aug-cc-pVTZ gas-phase excitation energy for *N*MB-TCNE complexes and experimental values in dependence on *N* (experimental values in gas phase are taken from [75, 76])

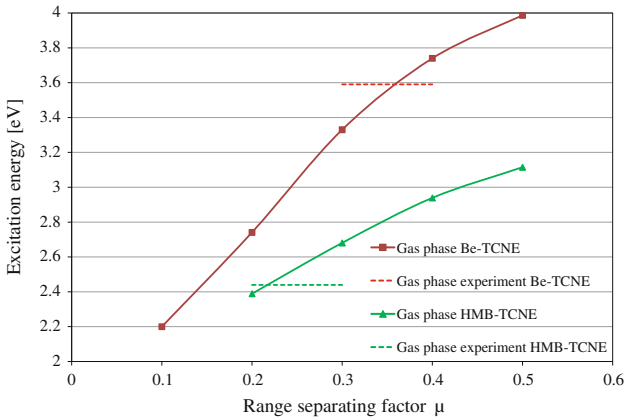

Fig. 5 Dependence of LC-BLYP/6-311+G(2d,p) excitation energy (for the first allowed transition) on value of range separating factor μ for benzene-TCNE and HMB-TCNE complexes

can be caused by an artefact of the theoretical calculation in which two perpendicular geometries of the complexes were considered with either the first or the second transition allowed. It can be also a consequence of decreased symmetry of mesitylene and HMB moieties in the complexes, due to presence of methyl groups. Finally, experimental determination of such small splitting is difficult since the absorption corresponds to two bands which are strongly overlapping, and thus, only an averaged dynamic absorption envelope is measured.

3.4 TD-LC-BLYP calculation of absorption transitions in NMB-TCNE

Above, we gave the reasons to use long-range corrected TD-DFT calculations with LC-BLYP functional. Thus, based on the acceptable result of the LC-BLYP method for transition energy in B-TCNE complex (with the range separating factor μ equal to 0.36, Fig. 5), one could hope

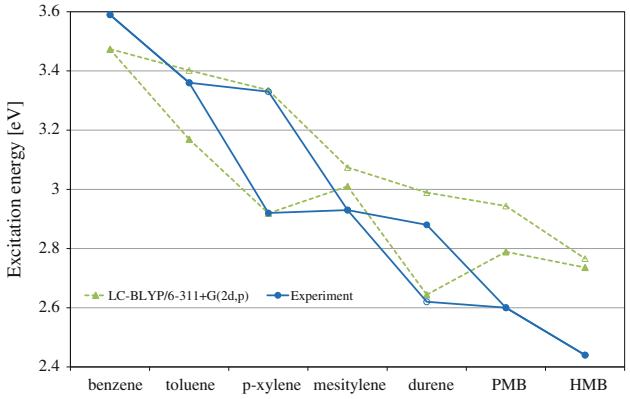

Fig. 6 LC-BLYP/6-311+G(2d,p) calculated excitation energies of *N*MB-TCNE complexes in gas phase and experimental values

that this relatively inexpensive approach might be a method of choice for further investigation of CT excitations in other *N*MB-TCNE complexes.

Unfortunately, the transition energy shows to be sensitively dependent on the range separation factor as can be seen in Fig. 5 for B-TCNE complex. For example, while the optimal value of this factor to fit experiment for the first transition in B-TCNE complex is 0.36, that for HMB-TCNE complex is established to be 0.22 (Fig. 5). Thus, to calculate transitions in all NMB-TCNE complexes, we have chosen the value $\mu = 0.33$. A comparison between LC-BLYP transition energies calculated with this factor and experimental values in the gas phase is given in Fig. 6 and indicates, in general, a reasonable agreement. Calculated splittings are in accord with experiment as well. However, the slope of the dependence of LC-BLYP excitation energies on *N* is significantly different from that of experimental data. This also implies that optimal value of separating factor is different for every *N*MB-TCNE complex, and thus, it does not have a general validity. Here, we also note that the increase of μ to, for example, the default Gaussian value (0.47) brings about too large increase of the excitation energy by ca. 0.5 eV. Therefore, for systematic and reliable analysis of a series of *N*MB-TCNE complexes, the CC2 method is clearly preferable to LC-BLYP. The latter could be a choice for larger CT complexes, for example, to establish trends in CT transitions in dependence on the structure of particular complexes.

3.5 Ionization potential versus transition energies in NMB-TCNE systems

OVGF calculated ionization potentials arising from the highest occupied MOs on particular methylated benzene versus *N* are plotted in Fig. 7. From the results, one can see that the dependence of *I*(*N*MB) on *N* is analogous to that of calculated transition energies as discussed before. Both the dependence of *I* values as well as the splitting between two highest occupied MO on number of methyl groups are similar to those found for the first two transition energies in the complexes. This follows from the simplified equation for the electron transition energy in CT complexes:

$$h\nu = I(N\text{MB}) - \text{EA}(\text{TCNE}) + C \quad (1)$$

where *I*(*N*MB) stands for respective ionization potential of *N*MB, *EA* is electron affinity of TCNE (3.17 ± 0.2 eV) [67], and *C* contains different terms originating from quantum chemical calculations where important one is the term expressing coulomb attraction between the amount of negative charge transferred to TCNE and respective positive hole on donor *N*MB molecule. However, the *C* term includes other contributions which are either constant or proportional to *I*(*N*MB). Figure 7 shows a strong correlation ($R^2 = 0.963$) between the above-mentioned quantities, however, with slope much lesser than one and equal to 0.73. This fact is caused mainly by depression (and its change with *N*) of the highest π-HOMOs in *N*MB-TCNE due to its interaction with π^*-LUMO on TCNE. The depression can be expressed by the equation which follows from simple perturbation theory

$$\begin{aligned}&\varepsilon_{\text{HOMO}}(\text{complex}) - \varepsilon_{\text{HOMO}}(\text{donor})\\ &\quad = \Delta\varepsilon \approx -(I_{\text{HOMO}}(\text{complex}) - I_{\text{HOMO}}(\text{donor}))\\ &\quad = -\frac{\langle \pi_{\text{HOMO}}|\hat{H}|\pi^*_{\text{LUMO}}\rangle^2}{\varepsilon_{\text{LUMO}} - \varepsilon_{\text{HOMO}}}\end{aligned} \quad (2)$$

where $\hat{H}$ is the Hamiltonian of the system. Since $\varepsilon_{\text{HOMO}}$ in respective donor increases with *N* due to the electron donor effect of methyl groups, the denominator in (2) decreases with *N*. Moreover, because of smaller interplanar distance with larger *N* and more intensive overlap between HOMO and LUMO, the nominator also increases with increasing *N*. Both the factors lead to the increase of $\Delta\varepsilon$ values (in absolute value) with increasing *N* and thus to the decrease of mentioned slope. It is also to say that respective ionization potential from HOMO in complex is larger than that in isolated donor.

3.6 Solvent effect on absorption transitions treated by PCM model

We calculated solvent effects by PCM model within CIS and LC-BLYP methods. The calculated PCM values show that the first two absorption transitions are shifted bathochromically by 0.25 eV for benzene-TCNE and 0.1 eV for HMB-TCNE complexes in CH_2Cl_2. The dependences of the solvent (CH_2Cl_2) red shift on the number of methyl groups *N* for experimental, CIS/PCM/aug-cc-pVDZ, and LC-BLYP/PCM/6-311+G(2d,p) values for the first transition energy in *N*MB-TCNE complexes are depicted in Fig. 8. From the figure, one can make several conclusions:

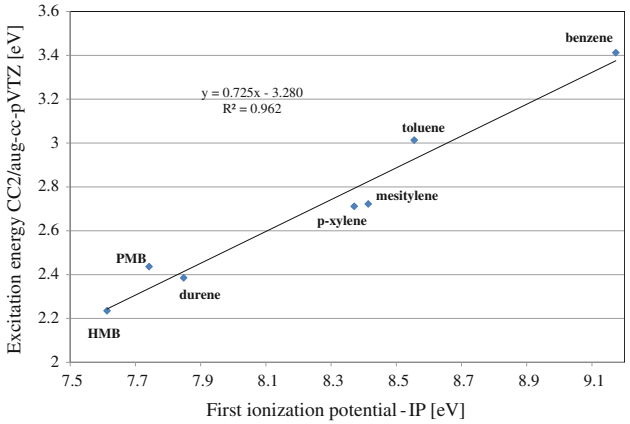

Fig. 7 Dependence of first absorption excitation energy in *N*MB-TCNE complexes on first ionization potential of *N*MB (OVGF/aug-cc-pVDZ calculations)

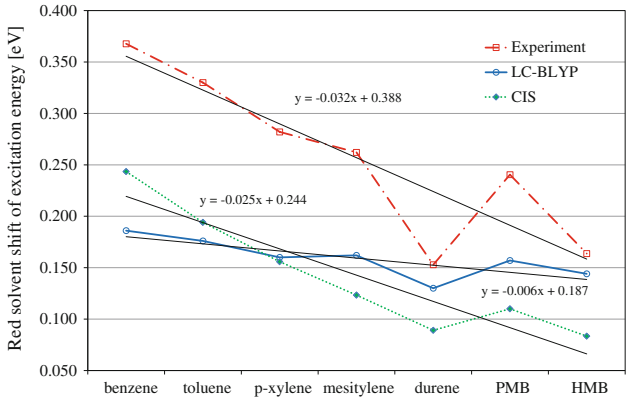

Fig. 8 The dependences of solvent red shift in CH_2Cl_2 solvent on the number of methyl groups *N* for the experimental, CIS/PCM/aug-cc-pVDZ, and LC-BLYP/PCM/6-311+G(2d,p) first transition energies in *N*MB-TCNE complexes

All three quantities almost linearly (with a few discrepancies) decrease with increasing *N* so that solvent red shifts are smaller at larger *N* (a straightforward explanation of this fact is based on electrostatics of PCM model—see further)

1. CIS/PCM red shift values are smaller by ca. 0.1–0.15 eV (depending on *N*) than experimental values, that is, smaller by ca. 30–40 %. The experimental and CIS/PCM curves have almost the same slope. The LC-BLYP/PCM values are in average comparable with the CIS/PCM values; however, the resulting dependence has a significantly smaller slope. This we regard as a general feature of TD-DFT approaches regardless of a functional used. Thus, for the treatment of solvent effects in CT complexes, the CIS/PCM approach is preferable to LC-BLYP/PCM.
2. As discussed above, the CC2/aug-cc-pVTZ values of studied CT transition energies are red-shifted with respect to experiment in the gas phase by ca. 0.2–0.15 eV. Since CIS/PCM/aug-cc-pVDZ underestimates the experimental solvent (CH_2Cl_2) red shifts by 0.1–0.15 eV, when the combined CC2 + CIS/PCM values together with experimental transition energies in CH_2Cl_2 are plotted against *N* (Fig. 9), one can observe almost full coincidence. This fact can be easily understood in the term of fortunate cancellation of the mentioned errors. The CC2 + CIS/PCM method can thus be advantageously exploited to treat quite accurately electronic absorptions of CT complexes in polar solvents of similar structures as those studied here. Moreover, since the red solvent shifts of absorption energy reach almost 70–80 % of their maximal value even in nonpolar solvents (see Fig. 10), the CC2 + CIS/PCM approach can also accurately describe CT transitions for these solvents.

The observed decrease of red shifts with increasing *N* can be explained through the PCM model: the increase of transferred electron charge (and correspondingly of the dipole moment) with increasing *N* (see entries in Table 2) in the ground states is accompanied by respective decrease of electron transfer in the excited states and, correspondingly, by the decrease of the excited state dipole moments. Greater electrostatic stabilization of the excited states compared to that of the ground states due to interaction with Franck–Condon induced charges on cavity surface thus leads to already discussed solvent red shift behaviour.

A sudden decrease of bathochromic shift for durene complex may be a consequence of several factors, for example, the near degeneration of the two highest HOMOs.

Data in Table 2 also indicate that while dipole moments and transferred electron charges (in parenthesis) from particular *N*MB to acceptor in the ground states increase with the number of methyl groups, in the excited states, the inverse trend is observed. Moreover, for each complex, the sum of electron charges transferred in the ground state and in the excited state is almost constant and equal to 1. The sum of respective dipole moments is also almost constant and approximately equal to 15 D, in accord with a simplified expression $1e^{-}R_{DA} \approx 14.4$ D (where R_{DA} is a typical interplanar distance between *N*MB-TCNE equal to 3.10^{-10} m).

The reason why the sum of transferred electron charges of the ground and excited states of particular *N*MB-TCNE complex is close to 1 is following: HOMO in GS of the complex is mainly represented by a linear combination of π-HOMO on isolated *N*MB and π^*-LUMO on isolated TCNE. The same is true for LUMO in the complex; however, here, the contribution from π^*-LUMO (on TCNE) is naturally dominating in such a way that the total contribution of either π-HOMO or π^*-LUMO of isolated components in HOMO and LUMO orbitals of the complex

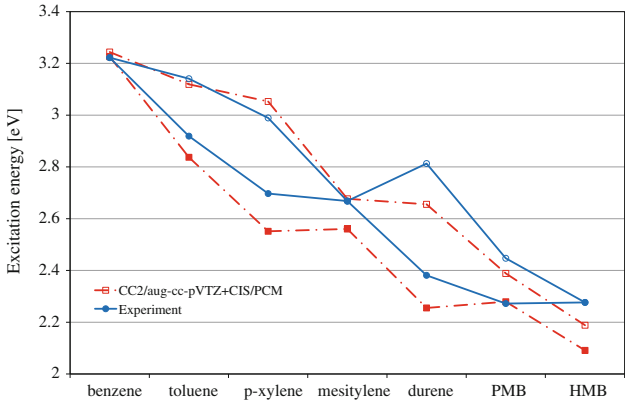

Fig. 9 Excitation energy of the first allowed transition in *N*MB-TCNE complexes. Theoretical CC2/aug-cc-pVTZ + CIS/aug-cc-pVDZ/PCM(CH_2Cl_2) results and experimental data measured in CH_2Cl_2 [69]

is approximately equal to one. As to solvent effect, polar CH_2Cl_2 solvent will stabilize more states with larger dipole moments (larger transferred electron charges) which causes that value of red solvent shifts is diminished with increasing number of methyl groups.

Short comments to entries in Table 2: "Nonequilibrium" solvation means that the CIS calculation is performed at the structure of the ground state (the Franck–Condon absorption transition) and with PCM induced charges in solvent which involve also correction for fast component of solvent polarization. Naturally, solute charges in the excited state are changed during such electronic CT transitions. "Equilibrium" solvation, in its turn, means that though geometry in the excited state is the same as that in the ground state, however, induced charges in the solvent are equilibrated according to the changed solute charges in particular excited state. Equilibration of solvent is very important, for example, for emission from the steady-state excited state to the ground state. To treat such emission, however, also geometry of the excited state has to be relaxed, that is, to be in energy minimum. As to dipole moments in equilibrated solvent induced charges, these are greater by 1.5–2 D in comparison with nonequilibrium

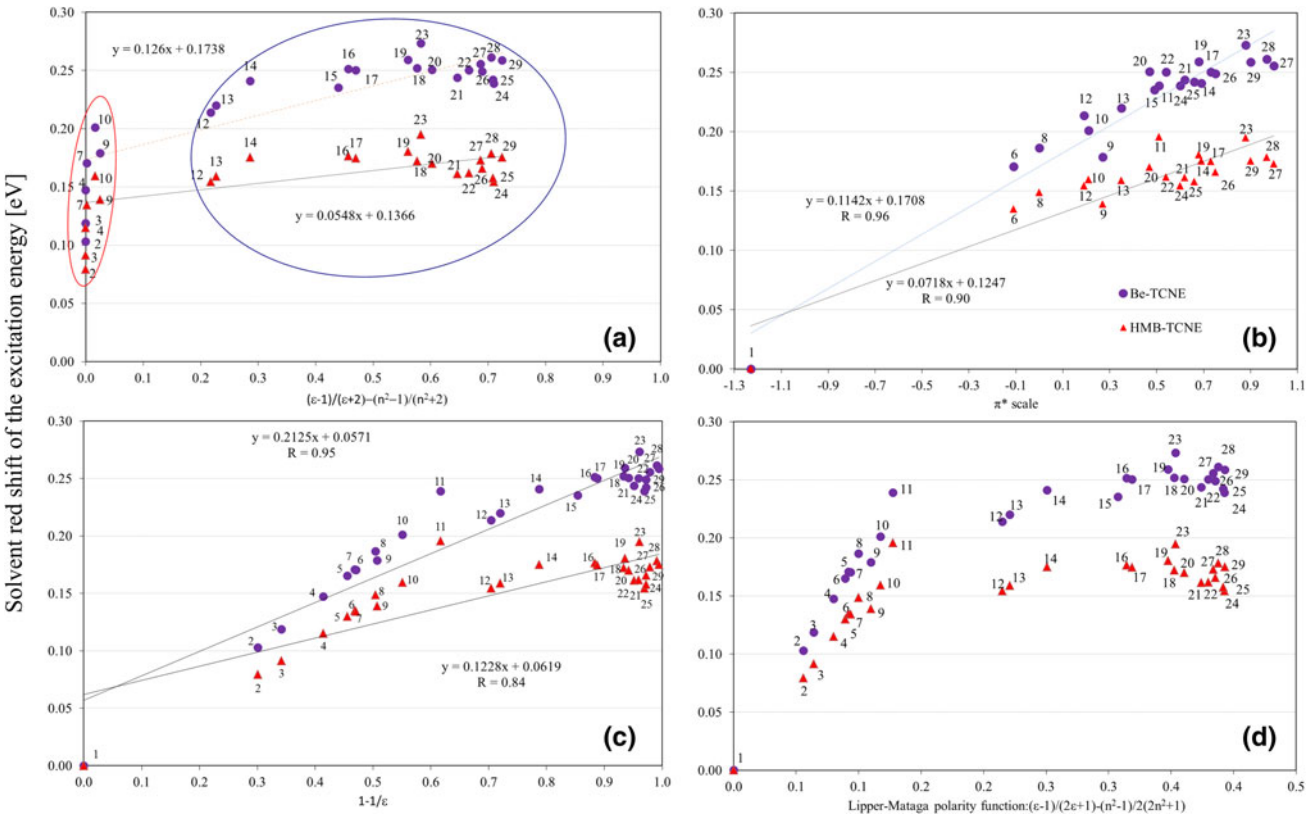

Fig. 10 Dependence of calculated excitation energy in B-TCNE complex on different polarity functions. Labelling of solvents: *1* gas phase, *2* argon, *3* krypton, *4* xenon, *5* n-pentane, *6* n-hexane, *7* 2-methylpentane, *8* cyclohexane, *9* hexafluorobenzene, *10* CCl_4, *11* CS_2, *12* diisopropyl ether, *13* diethylamine, *14* $CHCl_3$, *15* methylacetate, *16* 1-nonanol, *17* CH_2Cl_2, *18* 1-pentanol, *19* cyclohexanone, *20* 1-butanol, *21* acetone, *22* ethanol, *23* benzonitrile, *24* methanol, *25* acetonitrile, *26* nitromethane, *27* dimethyl sulfoxide, *28* formamide, *29* N-methylformamide

Table 2 Ground and excited state dipole moment (D) values in the gas phase and CH_2Cl_2 for *N*MB-TCNE complexes

N	Ground state		Excited state		
	Vacuum	CH_2Cl_2	Vacuum	Nonequilibrium solvation CH_2Cl_2	Equilibrium solvation CH_2Cl_2
0	1.72 (0.114e)[a]	1.63	12.03 (0.92e)[a]	12.98	14.53
1	2.03	1.96	11.77	12.72	14.32
2	2.24	2.27	11.39	12.41	14.10
3	2.36	2.11	11.49	12.58	14.30
4	2.48	2.58	11.51	12.60	14.31
5	2.94 (0.158e)[a]	3.14	11.31 (0.86)[a]	12.56	14.41
6	2.93	3.16	10.99	12.28	14.19

[a] Calculated transferred charges in parentheses

solvation. The reason for this is from the point of view of PCM model obvious.

3.6.1 *Solvent polarity effect on red shifts in excitation energy for B-TCNE and HMB-TCNE complexes*

Figure 10 contains data on CIS/PCM calculations of effect of solvents differing both in relative permittivity (ε) and in refractive index (n). It is well known that solvent shifts of electronic transitions depend both on relative permittivity and refractive index from which different polarity functions can be constructed. If we correlate the calculated CIS/PCM data for different solvents with the simplest polarity function $1–1/\varepsilon$, found plots indicate that even for non-polar solvents such as CCl_4 and cyclohexane, the red shifts values reach ca. 70–80 % of maximum values (Fig. 10c).

Figure 10a also contains the data of CIS/PCM red shifts but in dependence on more adequate polarity function, namely $((\varepsilon - 1)/(\varepsilon + 2)) - ((n^2 - 1)/(n^2 + 2))$, which contain both "slow", that is, reorientation and "fast", that is, dispersion polarizations (of the solvent) connected with Franck–Condon (FC) excitation. Again, even for modestly polar solvents, the red shifts are only by ca. 20–30 % less than the maximum values. Thus, when changing the gas phase, for example, for even slightly polar solvent such as CCl_4 and cyclohexane, the red shifts reach 70–80 % of its maximum value, and then—for more polar solvents—, the shifts do not change significantly. This means that in the non-equilibrium model, the (FC) excited state feels mainly the reaction field from the electron polarization of a solvent represented by the n^2 term. For all common solvents, this value varies only within a small interval, ca. from 1.8 (acetonitrile) to 2.2 (CCl_4). This is why the solvent shifts are not very sensitive to polarity. The reason why the red shifts for HMB-TCNE complex are smaller (see Fig. 10) than those for less methylated benzene-TCNE complexes was already discussed. Here, one can mention that the course of the red shift dependence for both HMB-TCNE and B-TCNE complexes on the same polarity function which contains both slow, that is, reorientation and fast, that is, dispersion polarizations of the solvent is very similar. Though, the shift values are smaller for the first complex (Fig. 10a) and the slopes of the dependences on polar solvents are almost the same.

The dependences of the solvent red shifts for B-TCNE and HMB-TCNE on another popular polarity function, namely that of Lippert-Mataga type (LM) [68] defined as $(\varepsilon - 1)/(2\varepsilon + 1) - (n^2 - 1)/2(2n^2 + 1)$, are shown in the Fig. 10d. It can be seen that the CIS/PCM red shift values plotted against the LM polarity function decompose into two groups according to solvent type: while the first group is formed by non-dipolar solvents, the second one contains dipolar solvents. Still, a general course of dependences on LM and just above-discussed polarity function is similar.

In this context, it is important to note that LM model [68] is based on approximation of solute as dipole immersed into a spherical cavity of polar medium, and thus, it uses the Onsager type of solvent polarization. On the other hand, the present work exploits the PCM model which considers correct multipole charge distribution of the solute and the realistic shape of cavity. When correlation between PCM calculated red shifts and the experimental π^* solvent polarity function [35] is tested, the linear dependences (with relevant correlation coefficients $R = 0.96$ and 0.90) are obtained for both B-TCNE and HMB-TCNE complexes and each of them, approximately, crossing the point with π^* value for the gas phase (Fig. 10b). This convinces us that the PCM model in principle correctly describes spectral solvent shifts for absorption transitions in the studied CT complexes. However, as stated before, the calculated red shifts are smaller by 30–40 % compared to experiment. This underestimation of red shifts is due to shortcomings of present PCM model; it can be attributed, for example, to significant lack of electronic correlation in CIS description of excited states relatively to the respective ground states and, partly, also to the absence of specific interactions between solvent and solute molecules, as well as actual parameterisation in the PCM approach used.

3.7 Oscillator strengths

Oscillator strength is an important property of all transitions; however, both quantum chemical calculations and experimental determination usually contain significant errors. On Fig. 11, there are depicted LC-BLYP values in dependence on the degree of methylation. One can observe that oscillator strength is significantly enhanced by increased number of methyls. This is caused by increased

HOMO–LUMO overlap since successive methylation decreases the distance between respective donor molecule and TCNE acceptor (Fig. 1). This is also to say that electron charge transfer in the ground state intensifies with increasing number of methyls. A significant and almost constant increase of f values calculated by the PCM model (Fig. 11) compared to the gas phase can be attributed to the fact that polar CH_2Cl_2 solvent enhances the electron transfer from *N*MB to TCNE (in the ground state of the complex) and thus also increases the overlap between the HOMO and LUMO orbitals.

Experimental f values are quite scattered depending on particular spectroscopic determination with averages ranging from 0.089 to 0.13 [69] for the first two absorption peaks. The lack of agreement between clearly increasing tendency of calculated f values on N and that of experimental values can be due to several factors related mainly to the change of interplanar distances in the solvent with respect to the gas phase as well as solvent effects on ε_{max} and half width of respective peak $\Delta\upsilon_{1/2}$.

3.8 Electronic transitions in 2:1 (2 HMB–TCNE) complex

In connection with still open question on reliability of experimental determination of EDA complexes with composition 2:1 (two donor molecules and one acceptor), we studied electronic transitions in the HMB_2-TCNE complex by the LC-BLYP/6-311+G(2d,p) method. Formation of this complex was postulated both in crystals [70] as well as in solution [71]. According to Liptay et al. [71], the equilibrium constant K_2 of the formation of the 2:1 complex arising from 1:1 complex, and HMB is about 20 $dm^3\ mol^{-1}$ while that of the 1:1 complex is much larger (190 $dm^3\ mol^{-1}$) in CCl_4. It is known that accuracy of experimental determination of the equilibrium constant for the 2:1 complex is rather problematic [72, 73]. This is particularly why theoretical studies on both electronic spectra and stability of the 2:1 complexes could be helpful. We carried out relatively time-consuming LC-BLYP/6-311+G(2d,p) calculations for this relatively large complex, and it was found that the interaction energy between the 1:1 complex and HMB (to form the 2:1 complex) is −75.5 kJ/mol, thus being appreciably lower than that for 1:1 complex (−92.1 kJ/mol) evaluated at the same level. This fact is in accord with the structural changes in these complexes: for example, the intermolecular distance between HMB and TCNE in the 1:1 parallel complex is 3.022 Å, while that in the 2:1 complex is larger and equal to 3.1 Å. These findings can be explained in terms of the repulsion between two HMB molecules present in the 2:1 complex. It is also worth noting that in crystals, the reverse order of the mentioned interplanar distances is observed:

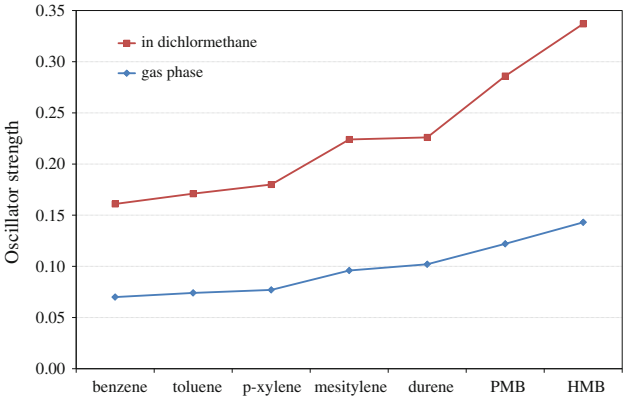

Fig. 11 Dependence of calculated absorption oscillator strength on the number of methyl groups in *N*MB-TCNE complexes

the 1:1 crystal has the averaged interplanar distance between HMB and TCNE planes equal to 3.28 Å [74] while that in the 2:1 crystal is shorter, being 2.98–3.18 Å. The explanation probably lies in the fact that in the solid state, there are, contrary to the gas phase, additional repulsive and attractive interactions between two directly faced HMB layers. This phenomenon is missing in the isolated 2:1 molecular complex.

From calculated LC-BLYP (with $\mu = 0.33$) electronic spectra of the 2:1 and 1:1 complexes, one can observe that two degenerated transitions from π-HOMO (HMB) → π^*-LUMO (TCNE) in two isolated 1:1 complexes (A, B—Scheme 2) are split (Davydov splitting) in the 2:1 complex due to formation of an exciton delocalized on both HMB units and the TCNE moiety. Analogous splitting is also observed for the second pair of degenerated π-HOMO-1 (HMB) → π^*-LUMO (TCNE) transitions, however, taken in geometry (orientation) in which both these latter transitions are allowed in the 1:1 complexes. However, due to exciton interaction in the 2:1 complex, only excitation with lower energy is allowed with almost twofold intensity. In Scheme 2, one can also see that the corresponding bathochromic shift of the first allowed exciton transition is equal to 0.06 eV, that is, 480 cm^{-1}.

From Scheme 2, it follows that due to mentioned splitting of two pairs of degenerated π-HOMOs in HMB donor molecules A and B, the four excited states arise. These come from four highest HOMOs in the complex denoted as φ_{1u}, φ_{2u}, φ_{3g}, and φ_{4g} (see Scheme 2) to $\varphi^*(\pi^*)$ orbital. The mentioned orbital φ originates from ± combinations of π-HOMO and π-HOMO-1 orbitals of the two isolated HMB molecules A and B (see Scheme 3). Only their ungerade (u) combinations could be allowed with regard to the centre of symmetry of the complex since π^*-LUMO is of gerade (g) symmetry (Scheme 3). However, also $\varphi_{1u} \rightarrow \pi^*$ is forbidden because of its respective irreducible representation within D_{2h} total symmetry of the 2:1

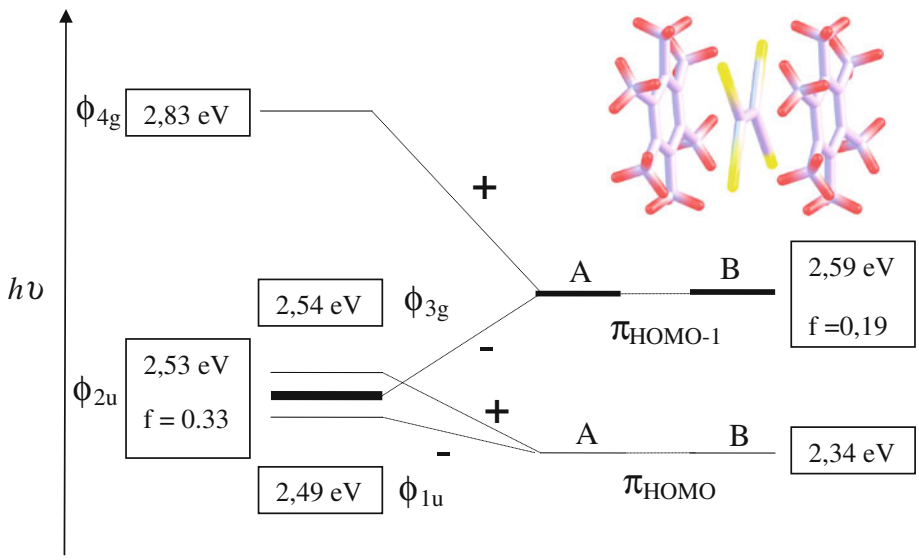

Scheme 2 Schematic LC-BLYP energy diagram of transitions $\varphi_i \rightarrow \pi^*$(LUMO) for the 2:1 complex HMB_2-TCNE (*left*). *Thick lines* stand for allowed transitions having with oscillator strength *f*, and *thin lines*, for forbidden transitions

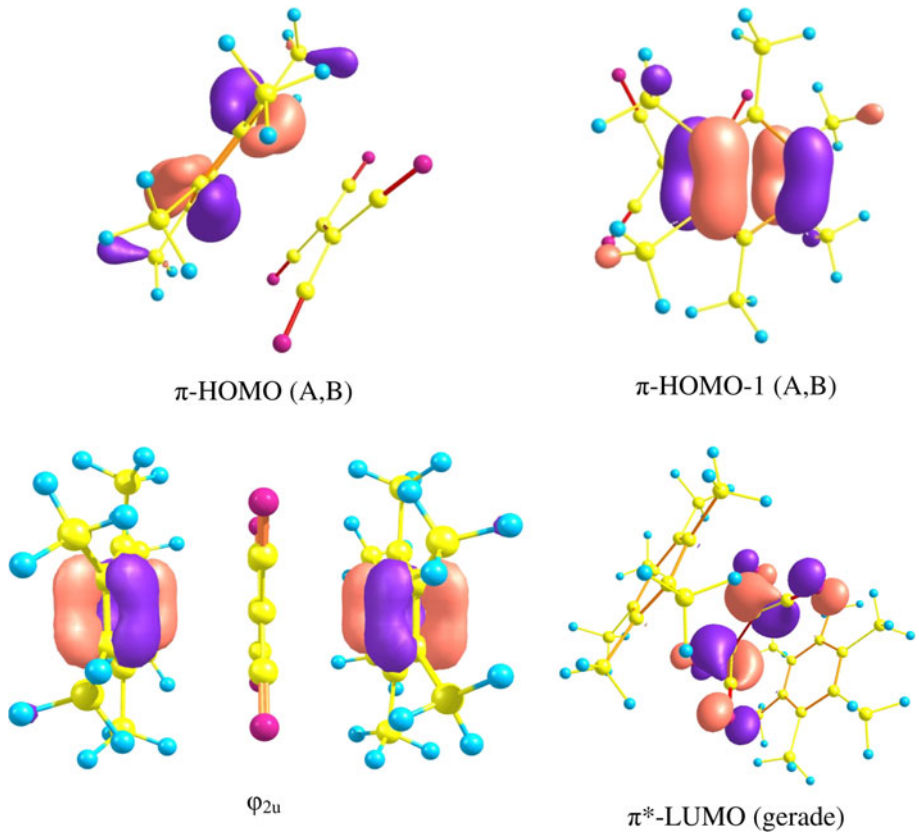

Scheme 3 Depiction of MO for π-HOMO, π-HOMO-1 in the 1:1 complex and φ_{2u}, π^*-LUMO in 2:1 complex

complex. Thus, the only allowed transition is $\varphi_{2u} \rightarrow \pi^*$ which has overlap density, consequently, of *u* symmetry. According to simplify consideration, the oscillator strength of this transition should be twice of that for π-HOMO-1 $\rightarrow \pi^*$ in the 1:1 complex. However, the calculated ratio is equal to 1.7 (i.e., 0.33/0.19), that is, it is slightly smaller. The difference certainly comes from a larger interplanar distance between donors and TCNE acceptor in the 2:1 complex compared to that in 1:1 complex (3.1 vs. 3.02 A). This fact leads to a smaller electron transition overlap density φ(HOMO) $\times$ π^*(LUMO) in the 2:1 complex, and thus, the smaller value of oscillator strength is obtained.

4 Conclusions

The paper brings new, accurate theoretical description of the charge-transfer (CT) electronic spectra of complete

series of all methylated benzenes-TCNE (*N*MB-TCNE) intermolecular EDA complexes and the detail comparison with experimental data both in the gas phase and in polar media so that solvent effects are studied in detail as well. It was shown that the transition energy of the first two (CT) absorption transitions in these *N*MB-TCNE is described well by the CC2/aug-cc-pVTZ method which, in agreement with experimental data, describes well both the bathochromic shift of the two π(NMB) $\rightarrow$ π*(TCNE) transitions (ranging from 3.41 to 2.23 eV) with the increasing number of methyl groups *N* as well as the value of splitting between them. Nevertheless, the CC2 transitions are systematically smaller, that is, red-shifted, with respect to experimental quantities in the gas phase by ca. 0.15–0.2 eV, which is an inaccuracy of this ab initio approach. Presented theoretical study of the first two singlet transitions in *N*MB-TCNE series of complexes thus shows that the RI-CC2/aug-cc-pVTZ approach is efficiently applied to describe CT transitions in this type of stacked complexes. The CC2 describes well both the bathochromic tendency of the two mentioned HOMOs (*N*MB) $\rightarrow$ LUMO (TCNE) transitions (ranging from 3.41 to 2.23 eV) with the number of methyl groups *N* as well as the splitting between them. The splitting ranges from 0.0 to 0.4 eV with zero values for symmetrical *N*MB, that is, for benzene, mesitylene, and HMB. Although the CC2/aug-cc-pVTZ method gives systematically lower transition energies by ca. 0.2–0.15 eV compared to experiment in the gas phase, due to underestimation of solvent red shifts in polar media by 0.15–0.1 eV by the CIS/PCM method in comparison with experiment, the combined CC2 + CIS/PCM approach can be considered as suitable to treat accurately electronic absorptions of larger CT complexes in polar solvents of similar structures as those studied here within the accuracy of 0.05 eV.

While LR-uncorrected GGA and hybrid DFT functionals fail to describe electronic transitions to excited states with significant CT character, we found that the TD-LC-BLYP method is able to treat such excitations in acceptable agreement with experiment.

Both CIS/PCM and LC-BLYP/PCM calculations predict red solvent shifts of all studied CT transitions in *N*MB-TCNE complexes. The shifts range from ca 0.25 to 0.1 eV in polar CH_2Cl_2 solvent. This tendency is explained in terms of the extent of electron transfer from particular *N*MB to TCNE in the ground and excited states and by the consequent electrostatic stabilization of these states in the polar solvent. Since the electron transfer in the ground state of *N*MB-TCNE complexes increases with increasing *N* and decreases in the case of their excited states, the stabilization of the ground state increases and that of the excited states decreases with the increase of *N*. As to much smaller solvent red shift found for TD-DFT/PCM approach in comparison with CIS/PCM approach, we regard it as a general feature of TD-DFT approaches regardless of a functional used. Thus, for the treatment of solvent effects, particularly, in CT complexes, the CIS/PCM approach is preferable to LC-BLYP/PCM.

Calculated values of the oscillator strength of the transitions in the studied complexes are in semi-quantitative agreement with the experimental data. However, while our calculations indicate the increase of *f* with increasing *N*, experimental results are rather scattered for different *N*.

TD-LC-BLYP study of the electronic spectra of the $(HMB)_2$-TCNE 2:1 complex indicates Davydov's exciton splitting. The splitting is due to electronic interaction in the exciton state, which arises from two local HOMO–LUMO excitations in both TCNE-HMB(A) and HMB(B)-TCNE moieties of the 2:1 complex. Both bathochromic shift of the allowed exciton transition as well as its ca. 1.6 times larger oscillator strength in the 2:1 complex compared to that in the 1:1 complex can be utilized in experimental studies of formation of the 2:1 complex from the 1:1 complex and HMB molecule.

Currently, we are thoroughly studying fluorescence of HMB-TCNE complex and comparing theoretical computations with available experimental data to explain unusual solvent shifts on the emission energies.

Acknowledgments This work has been financially supported by the Slovak Research and Development Agency (project No. APVV-0059-10) and VEGA grant No. 1/0524/11.

References

1. Foster R (1969) Organic charge-transfer complexes. Academic Press, New York
2. McGlynn SP (1958) Chem Rev 58:1113
3. Mulliken RS, Person WB (1969) Molecular complexes. Wiley, New York
4. Dega-Szafran Z, Kania A, Nowak-Wydra B, Szafran M (1994) J Mol Struct 322:223
5. Anelli PL, Ashton PR, Ballardini R, Balzani V, Delgado M, Gandolfi MT, Goodnow TT, Kaifer AE, Philp D (1992) J Am Chem Soc 114:193
6. Asakawa M, Ashton PR, Boyd SE, Brown CL, Gillard RE, Kocian O, Raymo FM, Stoddart JF, Tolley MS, White AJP, Williams DJ (1997) J Org Chem 62:26
7. Bissell RA, Cordova E, Kaifer AE, Stoddart JF (1994) Nature 369:133
8. Cordova E, Bissell RA, Kaifer AE (1995) J Org Chem 60:1033
9. Lokey RS, Iverson BL (1995) Nature 375:303
10. Toki A, Yonemura H, Matsuo T (1993) Bull Chem Soc Jpn 66:3382
11. Fox M, Chanon M (eds) (1988) Photoinduced electron transfer. Elsvier, New York
12. Amin AS, El-Beshbeshy AM (2001) Microchim Acta 137:63
13. Amin AS, Ahmed IS (2001) Microchim Acta 137:35
14. Kysel O, Juhasz G, Mach P, Kosik G (2007) Chem Pap 61:66

15. Kysel O, Budzak S, Medved M, Mach P (2008) Int J Quantum Chem 108:1533
16. Kysel O, Budzak S, Mach P, Medved M (2010) Int J Quantum Chem 110:1712
17. Stires JC, McLaurin EJ, Kubiak CP (2005) Chem Commun 41:3532
18. Headgordon M, Rico RJ, Oumi M, Lee TJ (1994) Chem Phys Lett 219:21
19. Christiansen O, Koch H, Jorgensen P (1995) Chem Phys Lett 243:409
20. Hattig C, Weigend F (2000) J Chem Phys 113:5154
21. Hellweg A, Grun SA, Hattig C (2008) Phys Chem Chem Phys 10:4119
22. Goerigk L, Grimme S (2010) J Chem Phys 132:184103
23. Rhee YM, Head-Gordon M (2007) J Phys Chem A 111:5314
24. Schirmer J (1982) Phys Rev A 26:2395
25. Grimme S, Neese F (2007) J Chem Phys 127:154116
26. Aquino AJA, Nachtigallova D, Hobza P, Truhlar DG, Hattig C, Lischka H (2011) J Comp Chem 32:1217
27. Kim HJ (1996) J Chem Phys 105:6818
28. Kim HJ (1996) J Chem Phys 105:6833
29. Amovilli C, Barone V, Cammi R, Cances E, Cossi M, Mennucci B, Pomelli CS, Tomasi J (1999) Adv Quant Chem 32:227
30. Aguilar MA, Delvalle FJO, Tomasi J (1993) J Chem Phys 98:7375
31. Mikkelsen KV, Cesar A, Agren H, Jensen HJA (1995) J Chem Phys 103:9010
32. Cammi R, Tomasi J (1995) Int J Quantum Chem 56:465
33. Mennucci B, Cammi R, Tomasi J (1998) J Chem Phys 109:2798
34. Cammi R, Frediani L, Mennucci B, Tomasi J, Ruud K, Mikkelsen KV (2002) J Chem Phys 117:13
35. Horng ML, Gardecki JA, Papazyan A, Maroncelli M (1995) J Phys Chem 99:17311
36. Grimme S (2006) J Comput Chem 27:1787
37. Jacquemin D, Laurent AD, Perpete EA, Andre JM (2009) Int J Quantum Chem 109:3506
38. Weigend F, Kohn A, Hattig C (2002) J Chem Phys 116:3175
39. Helgaker T, Klopper W, Koch H, Noga J (1997) J Chem Phys 106:9639
40. Tsuneda T, Kamiya M, Morinaga N, Hirao K (2001) J Chem Phys 114:6505
41. Dreuw A, Weisman JL, Head-Gordon M (2003) J Chem Phys 119:2943
42. Bernasconi L, Sprik M, Hutter J (2003) J Chem Phys 119:12417
43. Champagne B, Perpete EA, van Gisbergen SJA, Baerends EJ, Snijders JG, Soubra-Ghaoui C, Robins KA, Kirtman B (1998) J Chem Phys 109:10489
44. Tozer DJ, Handy NC (1998) J Chem Phys 109:10180
45. Iikura H, Tsuneda T, Yanai T, Hirao K (2001) J Chem Phys 115:3540
46. Wong BM, Piacenza M, Sala FD (2009) Phys Chem Chem Phys 11:4498
47. Jacquemin D, Perpete EA, Scuseria GE, Ciofini I, Adamo C (2008) Chem Phys Lett 465:226
48. Koopmans T (1933) Physica 1:104
49. Wv Niessen, Schirmer J, Cederbaum LS (1984) Comput Phys Rep 1:57
50. Cederbaum LS, Domcke W (1977) Adv Chem Phys 36:205
51. Tomasi J, Mennucci B, Cammi R (2005) Chem Rev 105:2999
52. Scalmani G, Frisch MJ (2010) J Chem Phys 132:114110
53. Frisch MJ, Trucks GW, Schlegel HB, Scuseria GE, Robb MA, Cheeseman JR, Scalmani G, Barone V, Mennucci B, Petersson GA, Nakatsuji H, Caricato M, Li X, Hratchian HP, Izmaylov AF, Bloino J, Zheng G, Sonnenberg JL, Hada M, Ehara M, Toyota K, Fukuda R, Hasegawa J, Ishida M, Nakajima T, Honda Y, Kitao O, Nakai H, Vreven T, Montgomery JA, Peralta JE, Ogliaro F, Bearpark M, Heyd JJ, Brothers E, Kudin KN, Staroverov VN, Kobayashi R, Normand J, Raghavachari K, Rendell A, Burant JC, Iyengar SS, Tomasi J, Cossi M, Rega N, Millam NJ, Klene M, Knox JE, Cross JB, Bakken V, Adamo C, Jaramillo J, Gomperts R, Stratmann RE, Yazyev O, Austin AJ, Cammi R, Pomelli C, Ochterski JW, Martin RL, Morokuma K, Zakrzewski VG, Voth GA, Salvador P, Dannenberg JJ, Dapprich S, Daniels AD, Farkas Ö, Foresman JB, Ortiz JV, Cioslowski J, Fox DJ (2009) Gaussian 09, revision A. 1. Gaussian. Gaussian, Inc., Wallingford, CT
54. Rappi AK, Casewit CJ, Colwell KS, Goddard WA, Skid WM (1992) J Am Chem Soc 114:10024
55. Cossi M, Barone V (2001) J Chem Phys 115:4708
56. Schmidt MW, Baldridge KK, Boatz JA, Elbert ST, Gordon MS, Jensen JH, Koseki S, Matsunaga N, Nguyen KA, Su SJ, Windus TL, Dupuis M, Montgomery JA (1993) J Comput Chem 14:1347
57. Ahlrichs R, Bar M, Haser M, Horn H, Kolmel C (1989) Chem Phys Lett 162:165
58. Karlstrom G, Lindh R, Malmqvist PA, Roos BO, Ryde U, Veryazov V, Widmark PO, Cossi M, Schimmelpfennig B, Neograd y P, Seijo L (2003) Comput Mater Sci 28:222
59. Klopper W, Manby FR, Ten-no S, Valeev EF (2006) Int Rev Phys Chem 25:427
60. Tsuzuki S, Honda K, Uchimaru T, Mikami M, Tanabe K (2000) J Am Chem Soc 122:3746
61. Tsuzuki S, Honda K, Uchimaru T, Mikami M, Tanabe K (2002) J Phys Chem A 106:4423
62. Hobza P, Selzle HL, Schlag EW (1996) J Phys Chem 100:18790
63. Antony J, Grimme S (2007) J Phys Chem A 111:4862
64. Granatier J, Pitonak M, Hobza P (2012) Accuracy of several wave function and density functional theory methods for description of noncovalent interaction of saturated and unsaturated hydrocarbon dimers. J Chem Theory Comput. doi:10.1021/ct300215p
65. Cramer CJ (2002) Essentials of computational chemistry: theories and models. John Wiley, New York
66. Peach MJG, Benfield P, Helgaker T, Tozer DJ (2008) J Chem Phys 128:044118
67. Chowdhury S, Kebarle P (1986) J Am Chem Soc 108:5453
68. Mataga N, Kaifu Y, Koizumi M (1956) Bull Chem Soc Jpn 29:465
69. Frey JE, Andrews AM, Ankoviac DG, Beaman DN, Dupont LE, Elsner TE, Lang SR, Zwart MAO, Seagle RE, Torreano LA (1990) J Org Chem 55:606
70. Pawlukojc A, Sawka-Dobrowolska W, Bator G, Sobczyk L, Grech E, Nowicka-Scheibe J (2006) Chem Phys 327:311
71. Liptay W, Rehm T, Wehning D, Schanne L, Baumann W, Lang W (1982) Z Naturforsch Teil A 37:1427
72. Smith ML, McHale JL (1985) J Phys Chem 89:4002
73. Zaini R, Orcutt AC, Arnold BR (1999) Photochem Photobiol 69:443
74. Maverick E, Trueblood KN, Bekoe DA (1978) Acta Crystallogr Sec B 34:2777
75. Hanazaki I (1972) J Phys Chem 76:1982
76. Merrifield RE, Phillips WD (1958) J Am Chem Soc 80:2778